# Reduced Basis Approximation and A Posteriori Error Estimation for the Time-Dependent Viscous Burgers Equation

**Cuong N. Nguyen[1], Gianluigi Rozza[1,⋆], Anthony T. Patera[1]**

Massachusetts Institute of Technology, Department of Mechanical Engineering, Room 3-264, 77 Mass Avenue, Cambridge MA, 02142-4307, USA; Email addresses: `cuongng@mit.edu`, `rozza@mit.edu`, `patera@mit.edu`

**Abstract.** In this paper we present rigorous *a posteriori* $L^2$ error bounds for reduced basis approximations of the unsteady viscous Burgers equation in one space dimension. The key new ingredient is accurate solution–dependent (Online) calculation of the exponential–in–time stability factor by the Successive Constraint Method. Numerical results indicate that the *a posteriori* error bounds are practicable for reasonably large times — many convective scales — and reasonably large Reynolds numbers — $O(100)$ or larger.

## 1. Introduction

The reduced basis method and related model–reduction approaches are well developed for linear parametrized parabolic partial differential equations [8,10,13,26,30]. However in the nonlinear case there are still many open research issues. We shall focus in this paper on the the development of rigorous *a posteriori* error bounds for the one–dimensional unsteady viscous Burgers equation. The latter is of interest primarily as a model for the unsteady incompressible Navier–Stokes equations, treatment of which — significantly complicated by the presence of the divergence–free condition — shall be considered in a subsequent paper. Although there are many examples of reduced order models for the unsteady incompressible Navier–Stokes equations [3,5,7,11,12, 15–19], none is endowed with rigorous *a posteriori* error bounds. (Note there are examples of rigorous reduced basis *a posteriori* error bounds for the *steady* Burgers [33] and incompressible Navier–Stokes [24,32] equations.)

The unsteady viscous Burgers equation, like the unsteady incompressible Navier–Stokes system, is in some sense computationally simple: a quadratic nonlinearity that admits standard Galerkin treatment. (Note for higher–order and non–polynomial nonlinearities more sophisticated reduced basis approximations must be considered [1,4,9,28] that in turn introduce both numerical and theoretical complications.) However, in the interesting case of small viscosity the unsteady viscous Burgers equation, like the unsteady incompressible Navier–Stokes system [6, 20], is also in some sense computationally very difficult: exponential instability compromises *a priori* and *a posteriori* error estimates — any *useful* bounds are perforce limited to modest (final) times and modest Reynolds numbers. (More precisely, stability considerations will limit the product of the final time and the Reynolds number.)

Our approach does not eliminate the exponential growth in time. (In some cases [20] it may be possible to demonstrate only algebraic growth in time; however, more generally — most simply, linearly unstable flows — we must admit exponential sensitivity to disturbances.) Rather we develop a procedure, within the reduced basis context, for the calculation of a more accurate (solution–dependent) estimate for the stability factor. The resulting error bounds, though certainly still pessimistic, are practicable for reasonably large (final) times — many convective scales — and reasonably large Reynolds number — O(100) or larger: meaningful application to many important "small" (lower Reynolds number) technologies, as well as to coarse–grained systems, may thus be possible. The error bounds can serve not only for certification, but also for efficient construction of rapidly convergent reduced basis approximations.

In Section 2 we introduce the reduced basis approximation for the unsteady viscous Burgers equation. In Section 3 we develop the associated *a posteriori* error bounds with particular emphasis on formulation and calculation of the stability growth factor. In Section 4 we summarize the Offline–Online computational strategy for efficient evaluation of the reduced basis output and output *a posteriori* error bound; we also describe our POD–Greedy sampling approach. Finally, in Section 5 we present numerical results. The latter are particularly important since the stability factors — and hence the utility of the bounds — can only be determined *in situ*.

## 2. Reduced Basis Approximation

To begin, we introduce the domain $\Omega =]0,1[$ and the space $X = H_0^1(\Omega)$, where $H_0^1(\Omega) = \{v \in H^1(\Omega) \,|\, v(0) = v(1) = 0\}$, $H^1(\Omega) = \{v \in L^2(\Omega) \,|\, v_x \in L^2(\Omega)\}$, and $L^2(\Omega) = \{v \text{ measurable} \,|\, \int_\Omega v^2 < \infty\}$. We further define the $X$ inner product and norm as $(w,v)_X = \int_\Omega w_x v_x$ and $\|w\|_X = \sqrt{(w,w)_X}$, respectively, and the $L^2(\Omega)$ inner product and norm as $(w,v) \equiv \int_\Omega wv$ and $\|w\| \equiv \sqrt{(w,v)}$, respectively. Finally, we introduce the closed parameter (viscosity) domain $\mathcal{D} \equiv [\nu_{\min}, \nu_{\max}]$ with $0 < \nu_{\min} < \nu_{\max}$.

We next introduce $L^2(\Omega)$–continuous linear functionals $f$ and $\ell$. Then, given $\nu \in \mathcal{D}$, $U(\nu) \in L^2(0,T;X) \cap C^0([0,T];L^2(\Omega))$ [29] satisfies

$$\frac{d}{dt}(U(t;\nu),v) + c(U(t;\nu),U(t;\nu),v) + \nu a(U(t;\nu),v) = f(v), \quad \forall v \in X, \tag{1}$$

with initial condition $U(t = 0;\nu) = 0$. We subsequently evaluate our "output of interest": for all times $t \in [0,T]$,

$$S(t;\nu) = \ell(U(t;\nu)). \tag{2}$$

Here $T$ is the final time, $C^0(I)$ is the space of continuous functions over the interval $I$, $\nu$ denotes the viscosity — we shall sometimes refer to $\nu^{-1}$ as the Reynolds number — and

$$\begin{aligned} c(w,z,v) &= -\frac{1}{2}\int_\Omega wzv_x, \\ a(w,v) &= \int_\Omega w_x v_x, \end{aligned} \tag{3}$$

are the convective trilinear and viscous bilinear forms, respectively. Equations (1) and (3) represent the standard unsteady viscous Burgers equation in one space dimension [23]; in our numerical experiments, we shall choose $f(v) = \int_\Omega v$.

We next introduce the time–discrete Burgers equation. Towards that end, we first divide the time interval $[0,T]$ into $K$ subintervals of equal length $\Delta t = T/K$; we then define $t^k \equiv k\Delta t$, $0 \le k \le K$. Given $\nu \in \mathcal{D}$, we now look for $u^k(\nu) \in X, 0 \le k \le K$, such that $u^0(\nu) = 0$ and

$$\frac{1}{\Delta t}(u^k(\nu) - u^{k-1}(\nu),v) + c(u^k(\nu),u^k(\nu),v) + \nu a(u^k(\nu),v) = f(v), \quad \forall v \in X, \tag{4}$$

for $1 \leq k \leq K$. We then evaluate the associated output: for $0 \leq k \leq K$,

$$s^k(\nu) = \ell(u^k(\nu)). \tag{5}$$

We shall sometimes denote $u^k(\nu)$ as $u(t^k; \nu)$ and $s^k(\nu)$ as $s(t^k; \nu)$ to more clearly identify the discrete time levels. Equation (4) – Euler Backward discretization of (1) — shall be our point of departure: we shall presume that $\Delta t$ is chosen sufficiently small that $u^k(\nu) = u(t^k; \nu)$ and $s^k(\nu) = s(t^k; \nu)$ are effectively indistinguishable from $U(t^k; \nu)$ and $S(t^k; \nu)$, respectively. (The development readily extends to Crank-Nicolson discretization; for purposes of exposition, we consider the simple Euler Backward approach.)

We next introduce a Galerkin finite element "truth" spatial discretization of our (already time–discrete) equation (4). We denote by $X^{\mathcal{N}}$ the standard conforming linear finite element space over a uniform "triangulation" of $\Omega$ comprising $\mathcal{N} + 1$ elements each of length $1/(\mathcal{N}+1)$; note that $X^{\mathcal{N}}$ is of dimension $\mathcal{N}$. Then, given $\nu \in \mathcal{D}$, we look for $u^{\mathcal{N}\,k}(\nu) \in X^{\mathcal{N}}, 0 \leq k \leq K$, such that $u^{\mathcal{N}\,0}(\nu) = 0$ and

$$\frac{1}{\Delta t}(u^{\mathcal{N}\,k}(\nu) - u^{\mathcal{N}\,k-1}(\nu), v) + c(u^{\mathcal{N}\,k}(\nu), u^{\mathcal{N}\,k}(\nu), v) + \nu a(u^{\mathcal{N}\,k}(\nu), v) = f(v), \quad \forall v \in X^{\mathcal{N}}, \tag{6}$$

for $1 \leq k \leq K$. We then evaluate the associated output: for $0 \leq k \leq K$,

$$s^{\mathcal{N}\,k}(\nu) = \ell(u^{\mathcal{N}\,k}(\nu)). \tag{7}$$

We shall build our reduced basis approximation upon the "truth" discretization (6), and we shall measure the error in our reduced basis prediction relative to $u^{\mathcal{N}\,k}(\nu) \equiv u^{\mathcal{N}}(t^k; \nu)$ and $s^{\mathcal{N}\,k}(\nu) \equiv s^{\mathcal{N}}(t^k; \nu)$. (As we shall observe, the Online cost of the reduced basis evaluations shall be independent of $\mathcal{N}$: we may thus choose $\mathcal{N}$ conservatively.)

Finally, we introduce the reduced basis approximation. Given a set of mutually $(\cdot, \cdot)_X$–orthonormal basis functions $\xi_n \in X^{\mathcal{N}}, 1 \leq n \leq N_{\max}$, the reduced basis spaces are given by

$$X_N \equiv \mathrm{span}\,\{\xi_n, 1 \leq n \leq N\}, \quad 1 \leq N \leq N_{\max}. \tag{8}$$

In actual practice (see Section 4), the spaces $X_N \in X^{\mathcal{N}}$ will be generated by a POD–Greedy sampling procedure which combines spatial snapshots in time and viscosity — $u^{\mathcal{N}\,k}(\nu)$ — in an optimal fashion; for our present purposes, however, $X_N$ can in fact represent any sequence of (low–dimensional) hierarchical approximation spaces [31]. Given $\nu \in \mathcal{D}$, we now look for $u_N^k(\nu) \in X_N, 0 \leq k \leq K$, such that $u_N^0(\nu) = 0$ and

$$\frac{1}{\Delta t}(u_N^k(\nu) - u_N^{k-1}(\nu), v) + c(u_N^k(\nu), u_N^k(\nu), v) + \nu a(u_N^k(\nu), v) = f(v), \quad \forall v \in X_N, \tag{9}$$

for $1 \leq k \leq K$. We then evaluate the associated output: for $0 \leq k \leq K$,

$$s_N^k(\nu) = \ell(u_N^k(\nu)). \tag{10}$$

We shall sometimes denote $u_N^k(\nu)$ as $u_N(t^k; \nu)$ and $s_N^k(\nu)$ as $s_N(t^k; \nu)$ to more clearly identify the discrete time levels. (Note that in fact all the reduced basis quantities should bear a $\mathcal{N}$ — $X_N^{\mathcal{N}}, u_N^{\mathcal{N}\,k}(\nu), s_N^{\mathcal{N}\,k}(\nu)$ — since the reduced basis approximation is defined in terms of a particular truth discretization; however, for clarity of exposition, we shall typically suppress the "truth" superscript.)

The goal of the reduced basis approximation is simple: dimension reduction — $N \ll \mathcal{N}$ — and associated computational economies. Obviously, for the Burgers equation in one space dimension, there is not much room for significant economies; however, in higher spatial dimensions, (Online) reduced basis evaluation is typically several orders of magnitude less expensive than the classical finite element approach [27,31].

### 3. *A Posteriori* Error Bound

*3.1. $L^2$ error bound*

In this section we aim to develop an *a posteriori* error bound $\Delta_N^k(\nu) \equiv \Delta_N(t^k; \nu), 1 \le k \le K$, for the $L^2$ error in the solution such that

$$\|u^{\mathcal{N} k}(\nu) - u_N^k(\nu)\| \le \Delta_N^k(\nu), \quad 1 \le k \le K, \quad \forall \nu \in \mathcal{D}, \tag{11}$$

for any $N = 1, \dots, N_{\max}$. Since the linear output functional $\ell$ is in $L^2(\Omega)$, the error in the output can then be bounded by

$$|s^{\mathcal{N} k}(\nu) - s_N^k(\nu)| \le \Delta_N^{s\,k}(\nu), \quad 1 \le k \le K, \forall \nu \in \mathcal{D}, \tag{12}$$

where $\Delta_N^{s\,k}(\nu)$ is the output error bound given by

$$\Delta_N^{s\,k}(\nu) = \left( \sup_{v \in X^{\mathcal{N}}} \frac{\ell(v)}{\|v\|} \right) \Delta_N^k(\nu). \tag{13}$$

We introduce the effectivities associated with these error estimates as

$$\eta_N(t^k; \nu) = \frac{\Delta_N^k(\nu)}{\|u^{\mathcal{N}k}(\nu) - u_N^k(\nu)\|} \quad \text{and} \quad \eta_N^s(t^k; \nu) = \frac{\Delta_N^{s\,k}(\nu)}{|s^{\mathcal{N} k}(\nu) - s_N^k(\nu)|}. \tag{14}$$

Clearly, the effectivities are a measure of the quality of the proposed estimator: for rigor, we shall insist upon effectivities $\ge 1$; for sharpness, we desire effectivities as close to unity as possible.

There are two main components to our error bounds. The first component is the dual norm of the residual

$$\varepsilon_N(t^k; \nu) = \sup_{v \in X^{\mathcal{N}}} \frac{r_N(v; t^k; \nu)}{\|v\|_X}, \quad 1 \le k \le K, \tag{15}$$

where $r_N(v; t^k; \nu)$ is the residual associated with the reduced basis approximation (9)

$$r_N(v; t^k; \nu) = f(v) - \frac{1}{\Delta t} \big( u_N^k(\nu) - u_N^{k-1}(\nu), v \big)$$
$$- c\big( u_N^k(\nu), u_N^k(\nu), v \big) - \nu a\big( u_N^k(\nu), v \big), \quad \forall v \in X^{\mathcal{N}}, \quad 1 \le k \le K. \tag{16}$$

Note the dual norm is defined over $X^{\mathcal{N}}$, and not $X$.

The second component is a lower bound

$$\rho_N^{\mathrm{LB}}(t^k; \nu) \le \rho_N(t^k; \nu), \quad 1 \le k \le K, \quad \forall \nu \in \mathcal{D}, \tag{17}$$

for the stability constant $\rho_N(t^k; \nu)$ defined as

$$\rho_N(t^k; \nu) = \inf_{v \in X^{\mathcal{N}}} \frac{4c\big( u_N^k(\nu), v, v \big) + \nu a(v, v)}{\|v\|^2}, \quad 1 \le k \le K, \quad \forall \nu \in \mathcal{D}. \tag{18}$$

The stability constant (18) is closely related to the absolute (monotonic decay) criterion of hydrodynamic stability theory [21]. If we assume that $u_N^k(\nu) \in L^{\infty}(\Omega), 1 \le k \le K$, it is a simple matter — application of Young's inequality to the first term in the numerator of (18) — to demonstrate that $\rho_N(t^k; \nu), 1 \le k \le K$, is well defined/bounded from below for any $\mathcal{N}(\to \infty)$. (Of course this characterization of $u_N^k(\nu)$ is crude and the corresponding bound pessimistic; in our actual estimation procedure, described in the next section, we reflect the full temporal–spatial structure of $u_N^k(\nu), 1 \le k \le K$.)

We can now define our error bound $\Delta_N^k(\nu), 1 \leq k \leq K$, in terms of the dual norm of the residual and the lower bound for the stability constant. We first define

$$\Delta t_N^*(\nu) = \frac{1}{|\min(0, \min_{1 \leq k \leq K} \rho_N^{\mathrm{LB}}(t^k; \nu))|}. \tag{19}$$

Then, for $\Delta t < \Delta t_N^*(\nu)$, we define our *a posteriori* error bound as

$$\Delta_N^k(\nu) = \sqrt{\frac{\frac{\Delta t}{\nu} \sum_{\ell=1}^k \left( \varepsilon_N^2(t^\ell; \nu) \prod_{j=1}^{\ell-1} \left( 1 + \Delta t \, \rho_N^{\mathrm{LB}}(t^j; \nu) \right) \right)}{\prod_{\ell=1}^k \left( 1 + \Delta t \, \rho_N^{\mathrm{LB}}(t^\ell; \nu) \right)}} \quad 1 \leq k \leq K. \tag{20}$$

Note (20) is simply the Euler Backward version of the standard continuous–time exponential result.

For $\nu$ sufficiently large (Reynolds sufficiently small), $\rho_N(t^k; \nu)$ will be uniformly positive and hence error growth will be controlled; in this case, we can consider rather large times — effectively reaching steady or (say) steady-periodic states. However, for smaller $\nu$, $\rho_N(t^k; \nu)$ will certainly be negative and hence the error bound (20) will grow exponentially in time; in this case, we will be practically limited to modest final times — the smaller the $\nu$, the smaller the practicable final time $T$. In fact, the actual limitations are less severe than might be anticipated: we shall quantify the restrictions for a particular example below. (Clearly, the $\nu^{-1/2}$ prefactor in the error bound (20) is also less than welcome; future work will consider different norms to attenuate this effect.)

To close this section we prove (11) for our bound of (20) by appropriate modification of standard procedures [29]:

**Proposition 1.** *For given $\nu \in \mathcal{D}$, $\Delta t < \Delta t_N^*(\nu)$, and error bound $\Delta_N^k(\nu)$ defined in (20), the error estimate (11) holds for any $N \in [1, N_{\max}]$.*

*Proof.* We note from (6) and (16) that the error $e^\ell(\nu) \equiv u^{\mathcal{N}\,\ell}(\nu) - u_N^\ell(\nu)$ satisfies

$$\frac{1}{\Delta t}\left(e^\ell(\nu) - e^{\ell-1}(\nu), v\right) + c\left(u^{\mathcal{N}\,\ell}(\nu), u^{\mathcal{N}\,\ell}(\nu), v\right) - c\left(u_N^\ell(\nu), u_N^\ell(\nu), v\right)$$
$$+ \nu a\left(e^\ell(\nu), v\right) = r_N(v; t^\ell; \mu), \quad \forall v \in X^{\mathcal{N}}. \tag{21}$$

From the definition of the trilinear form $c$ in (3) we can derive the following equality

$$c\left(u^{\mathcal{N}\,\ell}(\nu), u^{\mathcal{N}\,\ell}(\nu), v\right) - c\left(u_N^\ell(\nu), u_N^\ell(\nu), v\right) = c\left(e^\ell(\nu), e^\ell(\nu), v\right)$$
$$+ 2c\left(u_N^\ell(\nu), e^\ell(\nu), v\right), \quad \forall v \in X^{\mathcal{N}}. \tag{22}$$

It thus follows that

$$\frac{1}{\Delta t}\left(e^\ell(\nu) - e^{\ell-1}(\nu)(\nu), v\right) + c\left(e^\ell(\nu), e^\ell(\nu), v\right) + 2c\left(u_N^\ell(\nu), e^\ell(\nu), v\right)$$
$$+ \nu a\left(e^\ell(\nu), v\right) = r_N(v; t^\ell; \mu), \quad \forall v \in X^{\mathcal{N}}. \tag{23}$$

We now choose $v = e^\ell(\nu)$ in (23) and invoke (15) to find

$$\frac{1}{\Delta t} m\left(e^\ell(\nu) - e^{\ell-1}(\nu), e^\ell(\nu)\right) + c\left(e^\ell(\nu), e^\ell(\nu), e^\ell(\nu)\right)$$
$$+ 2c\left(u_N^\ell(\nu), e^\ell(\nu), e^\ell(\nu)\right) + \nu a\left(e^\ell(\nu), e^\ell(\nu)\right) \leq \varepsilon_N(t^\ell; \nu) \|e^\ell(\nu)\|_X. \tag{24}$$

Application of Young's inequality, $2AB \leq \frac{1}{\epsilon}A^2 + \epsilon B^2, \forall \epsilon > 0$, yields (for $\epsilon = \nu$)

$$\varepsilon_N(t^\ell; \nu)\|e^\ell(\nu)\|_X \leq \frac{1}{2}\left(\frac{1}{\nu}\varepsilon_N^2(t^\ell; \nu) + \nu\|e^\ell(\nu)\|_X^2\right)$$
$$= \frac{1}{2}\left(\frac{1}{\nu}\varepsilon_N^2(t^\ell; \nu) + \nu a\left(e^\ell(\nu), e^\ell(\nu)\right)\right). \tag{25}$$

We now note from the Cauchy-Schwarz and Young's inequalities that

$$\big(e^{\ell-1}(\nu), e^{\ell}(\nu)\big) \leq \frac{1}{2}\Big(\big(e^{\ell}(\nu), e^{\ell}(\nu)\big) + \big(e^{\ell-1}(\nu), e^{\ell-1}(\nu)\big)\Big); \tag{26}$$

we further note from (3) that

$$c\big(e^{\ell}(\nu), e^{\ell}(\nu), e^{\ell}(\nu)\big) = -\frac{1}{6}\int_0^1 \frac{\partial e^3(t^{\ell}; \nu)}{\partial x} = 0. \tag{27}$$

It thus follows from (24)-(27) that

$$\frac{1}{\Delta t}\Big(\big(e^{\ell}(\nu), e^{\ell}(\nu)\big) - \big(e^{\ell-1}(\nu), e^{\ell-1}(\nu)\big)\Big) + 4c\big(u_N^{\ell}(\nu), e^{\ell}(\nu), e^{\ell}(\nu)\big)$$
$$+ \nu a\big(e^{\ell}(\nu), e^{\ell}(\nu)\big) \leq \frac{1}{\nu}\varepsilon_N^2(t^{\ell}; \nu). \tag{28}$$

Hence, from (28) and (17)-(18) we obtain

$$\Big(1 + \Delta t\, \rho_N^{\mathrm{LB}}(t^{\ell}; \nu)\Big)\big(e^{\ell}(\nu), e^{\ell}(\nu)\big) - \big(e^{\ell-1}(\nu), e^{\ell-1}(\nu)\big) \leq \frac{\Delta t}{\nu}\varepsilon_N^2(t^{\ell}; \nu). \tag{29}$$

We now multiply by (the positive quantity, given our hypothesis on $\Delta t$) $\prod_{j=1}^{\ell-1}\big(1 + \Delta t\, \rho_N^{\mathrm{LB}}(t^j; \nu)\big)$ on both sides of (29) to obtain

$$\big(e^{\ell}(\nu), e^{\ell}(\nu)\big)\prod_{j=1}^{\ell}\big(1 + \Delta t\, \rho_N^{\mathrm{LB}}(t^j; \nu)\big) - \big(e^{\ell-1}(\nu), e^{\ell-1}(\nu)\big)\prod_{j=1}^{\ell-1}\big(1 + \Delta t\, \rho_N^{\mathrm{LB}}(t^j; \nu)\big) \leq$$
$$\frac{\Delta t}{\nu}\varepsilon_N^2(t^{\ell}; \nu)\prod_{j=1}^{\ell-1}\big(1 + \Delta t\, \rho_N^{\mathrm{LB}}(t^j; \nu)\big); \tag{30}$$

we then sum this equation from $\ell = 1$ to $k$ and recall $e(t^0; \nu) = 0$ to finally arrive at

$$\big(e^k(\nu), e^k(\nu)\big)\prod_{\ell=1}^{k}\Big(1 + \Delta t\, \rho_N^{\mathrm{LB}}(t^{\ell}; \nu)\Big) \leq$$
$$\frac{\Delta t}{\nu}\sum_{\ell=1}^{k}\varepsilon_N^2(t^{\ell}; \nu)\prod_{j=1}^{\ell-1}\big(1 + \Delta t\, \rho_N^{\mathrm{LB}}(t^j; \nu)\big), \quad 1 \leq k \leq K, \tag{31}$$

which is the desired result.

### 3.2. Successive Constraint Method

As already indicated, the theory (e.g., *a priori* or even *a posteriori* finite element error analysis) for the Navier-Stokes equations is plagued by exponential growth factors and large prefactors [6, 20]. (There are some cases in which algebraic-in-$T$ bounds can be derived [20], however the requisite conditions will not always be satisfied.) The simplest bounds for the exponential growth rate involve the $L^{\infty}(\Omega)$-norm of the gradient of the velocity — in our case, the gradient of $u_N(t; \nu)$ — which indeed will increase as $\nu^{-1/2}$ or $\nu^{-1}$ as $\nu$ decreases. We believe our formulation (20),(18), will improve upon these theoretical estimates, not enough to permit long-time integration at very high Reynolds numbers, but enough to permit practical and rigorous error estimation for (applications characterized by) modest times and modest Reynolds numbers.

There are two reasons for our optimism — admittedly bolstered in hindsight by the numerical results reported in a later section. First, (18) includes a viscous term that will somewhat constrain the minimizer and hence moderate the minimum — a candidate field large only in a thin destabilizing layer will also incur significant dissipation. Second, $\rho_N(t; \nu)$ of (18) shall be estimated (conservatively but) relatively precisely — our lower bound $\rho_N^{\mathrm{LB}}(t; \nu)$ shall reflect the detailed spatial and temporal structure of $u_N(t^k; \nu), 1 \leq k \leq K$. For the latter calculation we shall apply the Successive Constraint Method, as we now describe.

The Successive Constraint Method (SCM) introduced in [14,31] is a procedure for the construction of lower bounds for the coercivity and (in the non-coercive case) inf-sup stability constants that appear in our reduced basis *a posteriori* error bounds for linear elliptic (and parabolic) PDEs [31]. The SCM — based on an Offline-Online strategy relevant in the many-query and real–time reduced basis context — reduces the Online (real–time/deployed) calculation to a small Linear Program for which the operation count is independent of $\mathcal{N}$. The SCM method can in fact be applied to any generalized eigenproblem; we now consider adaption to the particular generalized eigenproblem of interest here — our stability constant (18).

*3.2.1. Preliminaries*  We first expand the reduced basis solution $u_N^k(\nu)$ as

$$u_N^k(\nu) = \sum_{n=1}^{N} \omega_{N\,n}(t^k; \nu)\xi_n, \tag{32}$$

where $\omega_N(t^k; \nu) = [\omega_{N\,1}(t^k; \nu), \ldots, \omega_{N\,N}(t^k; \nu)]^T \in \mathbf{R}^N$ is the reduced basis coefficient vector. We can thus write (18) as

$$\rho_N(t^k; \nu) = \inf_{v \in X^{\mathcal{N}}} \sum_{n=1}^{N+1} \Phi_N^n(t^k; \nu)\frac{d_N^n(v, v)}{\|v\|^2}, \tag{33}$$

where the symmetric bounded bilinear forms $d_N^n$ and the functions $\Phi_N^n(t^k; \nu)$ are given by

$$d_N^n(w, v) = \begin{cases} 2c(\xi_n, w, v) + 2c(\xi_n, v, w), & n = 1, \ldots, N, \\ a(w, v), & n = N + 1, \end{cases} \tag{34}$$

and

$$\Phi_N^n(t^k; \nu) = \begin{cases} \omega_{N\,n}(t^k; \nu), & n = 1, \ldots, N, \\ \nu, & n = N + 1. \end{cases} \tag{35}$$

It is important to note that the bilinear forms are independent of time and viscosity — this property shall be exploited in our development here.

For clarity of exposition, we introduce a time-parameter quantity $\mu = (t^k; \nu)$ in $\mathcal{D}^\mu \equiv \{t^0, \ldots, t^K\} \times \mathcal{D}$ (recall that $\mathcal{D} \equiv [\nu_{\min}, \nu_{\max}]$). We then introduce an objective function $\mathcal{J}_N^{\mathrm{obj}} : \mathcal{D}^\mu \times \mathbb{R}^{N+1} \to \mathbb{R}$ given by

$$\mathcal{J}_N^{\mathrm{obj}}(\mu; y) = \sum_{n=1}^{N+1} \Phi_N^n(\mu)y_n, \tag{36}$$

where $y = (y_1, \ldots, y_{N+1}) \in \mathbb{R}^{N+1}$. We may then express our stability constant as

$$\rho_N(\mu) = \inf_{y \in \mathcal{Y}_N} \mathcal{J}_N^{\mathrm{obj}}(\mu; y), \tag{37}$$

where the set $\mathcal{Y}_N \subset \mathbb{R}^{N+1}$ is defined by

$$\mathcal{Y} = \left\{ y \in \mathbb{R}^{N+1} \mid \exists w_y \in X^{\mathcal{N}} \text{ s.t. } y_n = \frac{d_N^n(w_y, w_y)}{\|w_y\|^2}, \ 1 \leq n \leq N + 1 \right\}. \tag{38}$$

The equivalence between (33) and (37), (38) is readily confirmed.

We now introduce the "continuity constraint" box

$$\mathcal{B}_N = \prod_{n=1}^{N+1} \left[ \inf_{w \in X^{\mathcal{N}}} \frac{d_N^n(w,w)}{\|w\|_X^2}, \sup_{w \in X^{\mathcal{N}}} \frac{d_N^n(w,w)}{\|w\|_X^2} \right]; \tag{39}$$

from continuity of the $d_N^n, 1 \leq n \leq N+1$, $\mathcal{B}_N$ shall be bounded. We further assume that we are given the SCM sample

$$\mathcal{C}_J = \{\mu_1^{\mathrm{SCM}} \in \mathcal{D}^\mu, \ldots, \mu_J^{\mathrm{SCM}} \in \mathcal{D}^\mu\}; \tag{40}$$

selection of the sample points $\mu_j^{\mathrm{SCM}}, 1 \leq j \leq J$, shall be discussed subsequently. We denote by $\mathcal{C}_J^{M,\mu}$ the set of $M$ ($\geq 1$) points in $C_J$ closest to a given $\mu \in \mathcal{D}^\mu$. We measure proximity in a weighted norm: for $\mu = (t^k; \nu) \in \mathcal{D}^\mu$ and $\mu' = (t^{k'}; \nu') \in C_J$, the distance between $\mu$ and $\mu'$ is defined as

$$\mathrm{dist}(\mu, \mu') = \sqrt{(T(\nu - \nu'))^2 + (\nu(t^k - t^{k'}))^2}; \tag{41}$$

this choice will ensure that the set $\mathcal{C}_J^{M,\mu}$ contains many points nearby $\nu$. (Note that if $M > J$, then we set $\mathcal{C}_J^{M,\mu} = \mathcal{C}_J$.)

*3.2.2. Lower Bound* Now for given $\mathcal{C}_J$, $M \in \mathbb{N} \equiv \{1, 2, \ldots\}$, and any $\mu \in \mathcal{D}^\mu$, we define the "lower bound" set $\mathcal{Y}_N^{\mathrm{LB}}(\mu; \mathcal{C}_J, M) \subset \mathbb{R}^{N+1}$ as

$$\mathcal{Y}_N^{\mathrm{LB}}(\mu; \mathcal{C}_J, M) \equiv \left\{ y \in \mathbb{R}^{N+1} \mid y \in \mathcal{B}_N , \sum_{n=1}^{N+1} \Phi_N^n(\mu') y_q \geq \rho_N(\mu'), \forall \mu' \in \mathcal{C}_J^{M,\mu} \right\}. \tag{42}$$

We then define our lower bound

$$\rho_N^{\mathrm{LB}}(\mu; \mathcal{C}_J, M) = \min_{y \in \mathcal{Y}_N^{\mathrm{LB}}(\mu; \mathcal{C}_J, M)} \mathcal{J}_N^{\mathrm{obj}}(\mu; y). \tag{43}$$

We can demonstrate [14,31] that $\mathcal{Y}_N \subset \mathcal{Y}_N^{\mathrm{LB}}(\mu; \mathcal{C}_J, M)$ and hence

**Proposition 2.** *Given $\mathcal{C}_J \subset \mathcal{D}^\mu$ and $M \in \mathbb{N}$,*

$$\rho_N^{\mathrm{LB}}(\mu) \leq \rho_N(\mu), \quad \forall \mu \in \mathcal{D}^\mu, \tag{44}$$

*for $\rho_N^{\mathrm{LB}}(\mu = (t^k; \mu)) = \rho_N^{\mathrm{LB}}(\mu; \mathcal{C}_J, M)$ defined in (43).*

We note that our lower bound (43) is in fact a linear optimization problem (or Linear Program (LP)). We observe that our LP (43) contains $N+1$ design variables and $2(N+1) + M$ (one-sided) inequality constraints. The crucial observation is that the operation count to evaluate $\mu \rightarrow \rho_N^{\mathrm{LB}}(\mu)$, *given* $\mathcal{B}_N$ and the set $\{\rho_N(\mu') \mid \mu' \in \mathcal{C}_J\}$, is *independent* of $\mathcal{N}$; we discuss the Offline–Online computational implications in the next section.

*3.2.3. Upper Bound* As we shall see, we also require an *upper* bound for the coercivity constant for the (effective) construction of a good "coercivity constraint" sample $\mathcal{C}_J$. For given $\mathcal{C}_J, M \in \mathbb{N}$, and any $\mu \in \mathcal{D}^\mu$, we introduce our "upper bound" set $\mathcal{Y}_N^{\mathrm{UB}}(\mu; \mathcal{C}_J, M)$ as

$$\mathcal{Y}_N^{\mathrm{UB}}(\mu; \mathcal{C}_J, M) = \left\{ y^*(\mu') \mid \mu' \in \mathcal{C}_J^{M,\mu} \right\}, \tag{45}$$

where

$$y^*(\mu) = \arg \inf_{y \in \mathcal{Y}_N} \mathcal{J}_N^{\mathrm{obj}}(\mu; y)$$

(in the event of non-uniqueness, any selection criterion suffices). We can then define our upper bound as

$$\rho_N^{\mathrm{UB}}(\mu; \mathcal{C}_J, M) = \min_{y \in \mathcal{Y}_N^{\mathrm{UB}}(\mu; \mathcal{C}_J, M)} \mathcal{J}_N^{\mathrm{obj}}(\mu; y). \tag{46}$$

It directly follows from (45) that $\mathcal{Y}_N^{\mathrm{UB}}(\mu; \mathcal{C}_J, M) \subset \mathcal{Y}_N$ and hence, for given $\mathcal{C}_J$ and $M \in \mathbb{N}$, $\rho_N^{\mathrm{UB}}(\mu; \mathcal{C}_J, M) \geq \rho_N(\mu), \forall \mu \in \mathcal{D}^\mu$.

We note that the upper bound (46) is a simple enumeration: *given* the set $\{y^*(\mu') \mid \mu' \in \mathcal{C}_J\}$, the operation count to evaluate $\mu \rightarrow \rho_N^{\mathrm{UB}}(\mu)$ is *independent* of $\mathcal{N}$. We return to the computational implications shortly.

*3.2.4. Greedy Selection of $\mathcal{C}_J$* We now present the construction of the set $\mathcal{C}_J$ by a greedy algorithm. We shall require a "train" sample $\Xi_{\mathrm{train,SCM}} = \{\mu_1^{\mathrm{train,SCM}}, \ldots, \mu_{n_{\mathrm{train,SCM}}}^{\mathrm{train,SCM}}\} \subset \mathcal{D}^\mu$ of $n_{\mathrm{train,SCM}}$ points. We also require a tolerance $\epsilon_{\mathrm{SCM}}$ of the order of unity which shall control the error in the lower bound prediction.

We first set $J = 1$ and choose $\mathcal{C}_1 = \{\mu_1^{\mathrm{SCM}}\}$ "arbitrarily." We then perform

$$\texttt{While} \max_{\mu \in \Xi_{\mathrm{train,SCM}}} \left[ \frac{\exp(T\,\rho_{N_{\max}}^{\mathrm{UB}}(\mu; \mathcal{C}_J, M)) - \exp(T\,\rho_{N_{\max}}^{\mathrm{LB}}(\mu; \mathcal{C}_J, M))}{\exp(T\,\rho_{N_{\max}}^{\mathrm{LB}}(\mu; \mathcal{C}_J, M))} \right] > \epsilon_{\mathrm{SCM}} :$$

$$\mu_{J+1}^{\mathrm{SCM}} = \arg \max_{\mu \in \Xi_{\mathrm{train,SCM}}} \left[ \frac{\exp(T\,\rho_{N_{\max}}^{\mathrm{UB}}(\mu; \mathcal{C}_J, M)) - \exp(T\,\rho_{N_{\max}}^{\mathrm{LB}}(\mu; \mathcal{C}_J, M))}{\exp(T\,\rho_{N_{\max}}^{\mathrm{LB}}(\mu; \mathcal{C}_J, M))} \right] ;$$

$$\mathcal{C}_{J+1} = \mathcal{C}_J \cup \mu_{J+1}^{\mathrm{SCM}} ;$$

$$J \leftarrow J + 1 ;$$

$$\texttt{end.}$$

We denote by $J^{\max}(\epsilon_{\mathrm{SCM}})$ the value of $J$ upon exit — the value of $J$ for which our tolerance is satisfied: our lower bound for $N = N_{\max}$ is thus given by $\rho_{N_{\max}}^{\mathrm{LB}}(\mu = (t^k; \mu)) = \rho_{N_{\max}}^{\mathrm{LB}}(\mu; \mathcal{C}_{J^{\max}}, M)$. Note we control not the gap between the upper bound and the lower bound but rather the gap between the exponential of the upper bound and the exponential of the lower bound: this heuristic better reflects the effect of the stability parameter on the ultimate $L^2$ *a posteriori* error bound. We typically choose $\epsilon_{\mathrm{SCM}} = T\nu_{\max}$.

It is important to note that our greedy algorithm is performed for $N = N_{\max}$. Then, once the SCM sample has been constructed, we compute the $\rho_N(\mu_j^{\mathrm{SCM}}), 1 \leq j \leq J^{\max}$, for all $N = 1, \ldots, N_{\max} - 1$. (Note that the $\rho_{N_{\max}}(\mu_j^{\mathrm{SCM}}), 1 \leq j \leq J^{\max}$, are already calculated as part of the greedy procedure.) We can thus evaluate $\rho_N^{\mathrm{LB}}(\mu) = \rho_N^{\mathrm{LB}}(\mu; \mathcal{C}_{J^{\max}}, M)$ from (43) — and Proposition 2 remains valid — for any $N \in [1, N_{\max}]$ and any $\mu \in \mathcal{D}^\mu$. Of course, our tolerance $\epsilon_{\mathrm{SCM}}$ may not be precisely satisfied for all $N$, and in particular smaller $N$; however, for the larger $N$ of interest, the greedy selection ensures a sufficiently good lower bound.

Finally, we close by noting that SCM calculation of the nonlinear Burgers stability factor is particularly demanding: the number of terms in the affine expansion of the objective function increases with $N$, the dimension of the reduced basis approximation space. (In contrast, for linear problems, the coercivity and inf–sup stability factors depend only on the parametric form of the associated PDE operator.) As a result, we can expect (and we will confirm) that $J^{\max}$ will not be too small. However, it is important to note that the spectrum of the reduced basis solution — the $\omega_{N\,n}^k, 1 \leq n \leq N$ — will decay very quickly, and hence the variation in the $\Phi_N^n(t^k; \nu)$ will be quite small: this partially mitigates the effects of increasing dimensionality.

## 4. Offline–Online Computational Approach

### 4.1. Construction–Evaluation Decomposition

The calculation of the reduced basis output $s_N(t^k; \nu)$ and output error bound $\Delta_N^s(t^k; \nu)$ admits a Construction–Evaluation decomposition. The expensive — $\mathcal{N}$–dependent — Construction stage, performed once, enables the subsequent very inexpensive — $\mathcal{N}$–independent — Evaluation stage, performed many times for each new desired $\nu \in \mathcal{D}$. Note the reduced basis approach is

particularly relevant in the real–time context and the many–query context; for the former the relevant metric is marginal cost — the (inexpensive) Evaluation stage — while for the latter the relevant metric is asymptotic average cost — again, the (inexpensive) Evaluation stage. We first discuss the Construction–Evaluation approach for $s_N(t^k; \nu), 1 \le k \le K$; we subsequently discuss the Construction–Evaluation approach for the output error bound $\Delta_N^s(t^k; \nu)$.

In order to compute $s_N(t^k; \nu)$ we expand $u_N(t^k; \nu), 1 \le k \le K$, as

$$u_N(t^k; \nu) = \sum_{j=1}^{N} \omega_{N\,j}^k(\nu) \xi_j, \tag{47}$$

where we recall that the $\xi_j, 1 \le j \le N$, are the basis functions for our reduced basis space $X_N$. We may then evaluate the reduced basis output as

$$s_N(t^k; \nu) = \sum_{j=1}^{N} \omega_{N\,j}^k(\nu) \ell(\xi_j), \quad 1 \le k \le K. \tag{48}$$

It remains to obtain the $\omega_{N\,j}^k(\nu), 1 \le j \le N, 1 \le k \le K$.

At any given time level $t^k$, we find $u_N(t^k; \nu)$ from Newton iteration applied to (9): if we denote the current Newton iterate as $\overline{u}_N(t^k; \nu)$ then the Newton increment $\delta u_N(t^k; \nu)$ satisfies

$$\frac{1}{\Delta t}(\delta u_N(t^k; \nu), v) + 2c(\overline{u}_N(t^k; \nu), \delta u_N(t^k; \nu), v) + \nu a(\delta u_N(t^k; \nu), v) = \overline{r}_N(v; t^k; \nu), \quad \forall v \in X_N, \tag{49}$$

where for all $v \in X_N$ (or $X^{\mathcal{N}}$) the Newton residual is given by

$$\begin{aligned} \overline{r}_N(v; t^k; \nu) \equiv f(v) &- \frac{1}{\Delta t}(\overline{u}_N(t^k; \nu) - u_N(t^{k-1}; \nu), v) \\ &- c(\overline{u}_N(t^k; \nu), \overline{u}_N(t^k; \nu), v) - \nu a(\overline{u}_N(t^k; \nu), v) \end{aligned}. \tag{50}$$

The next iterate is then given by $\overline{u}_N(t^k; \nu) + \delta u_N(t^k; \nu)$; we continue until convergence. We now express the crucial computational kernel — (49) and (50) — in algebraic form.

Towards that end, we first expand the current Newton iterate and the Newton increment as

$$\overline{u}_N(t^k; \nu) = \sum_{j=1}^{N} \overline{\omega}_{N\,j}^k(\nu) \xi_j, \tag{51}$$

$$\delta u_N(t^k; \nu) = \sum_{j=1}^{N} \delta \omega_{N\,j}^k(\nu) \xi_j, \tag{52}$$

respectively. It then follows from (49) and (50) that the $\delta \omega_{N\,j}^k(\nu), 1 \le j \le N$, satisfy the equations

$$\sum_{j=1}^{N} \left[ \frac{\mathcal{M}_{N\,ij}}{\Delta t} + 2 \sum_{n=1}^{N} \overline{\omega}_{N\,n}^k(\nu) \mathcal{C}_{N\,nij} + \nu \mathcal{A}_{N\,ij} \right] \delta \omega_{N\,j}^k(\nu) = \overline{r}_N(\xi_i; t^k; \nu), \quad 1 \le i \le N, \tag{53}$$

with

$$\begin{aligned} \overline{r}_N(\xi_i; t^k; \nu) = f(\xi_i) &- \sum_{j=1}^{N} \frac{\mathcal{M}_{N\,ij}}{\Delta t}(\overline{\omega}_{N\,j}^k(\nu) - \omega_{N\,j}^{k-1}(\nu)) \\ &- \sum_{n=1}^{N} \sum_{j=1}^{N} \mathcal{C}_{N\,nij} \overline{\omega}_{N\,n}^k(\nu) \overline{\omega}_{N\,j}^k(\nu) - \nu \sum_{j=1}^{N} \mathcal{A}_{N\,ij} \overline{\omega}_{N\,j}^k(\nu), \end{aligned} \tag{54}$$

10

for $1 \leq i \leq N$. Here the

$$\mathcal{M}_{N\,ij} = (\xi_j, \xi_i), \quad \mathcal{C}_{N\,nij} = c(\xi_n, \xi_j, \xi_i), \quad \mathcal{A}_{N\,ij} = a(\xi_j, \xi_i), \quad 1 \leq i, j, n \leq N, \qquad (55)$$

are parameter–independent arrays. We can now readily identify the Construction–Evaluation decomposition.

In the *Construction* stage we first form and store the time–independent and $\nu$–independent arrays $\mathcal{M}_{N_{\max}\,ij}, \mathcal{C}_{N_{\max}\,nij}, \mathcal{A}_{N_{\max}\,ij}, f(\xi_i)$, and $\ell(\xi_i), 1 \leq n, i, j \leq N_{\max}$. The operation count in the Construction stage of course depends on $\mathcal{N}$ — even once the $\xi_i, 1 \leq i \leq N_{\max}$, are *known* (obtained by the sampling procedure of the next section), it remains to compute $O(N_{\max}^3)$ finite element quadratures over the triangulation. Note that, thanks to the hierarchical nature of the reduced basis spaces, the stiffness matrices/vectors $\mathcal{M}_{N\,ij}, \mathcal{C}_{N\,nij}, \mathcal{A}_{N\,ij}, f(\xi_i)$, and $\ell(\xi_i), 1 \leq n, i, j \leq N$, for any $N \leq N_{\max}$ can be extracted as principal subarrays of the corresponding $N_{\max}$ quantities. (For nonhierarchical reduced basis spaces the storage requirements are much higher.)

In the *Evaluation* stage, for each Newton iteration at each time level $k = 1, \ldots, K$: we first form the left–hand side of (53) and the residual of (54) — in $O(N^3)$ operations; we then solve the resulting $N \times N$ system of linear equations for $\delta\omega_{N\,j}^k, 1 \leq j \leq N$ — again in $O(N^3)$ operations (in general, we must anticipate that the reduced basis matrices will be dense). Once the $\omega_{N\,j}^k, 1 \leq j \leq N, 1 \leq k \leq K$, are obtained — $O(N^3 K)$ operations in total — we evaluate our output from (48) — in $O(NK)$ operations. The storage and operation count in the Evaluation stage is clearly independent of $\mathcal{N}$, and we can thus anticipate — presuming $N \ll \mathcal{N}$ — very rapid reduced basis response in the real–time and many–query contexts (at least for problems in higher space dimensions).

We now turn to the error bound $\Delta_N^s(t^k; \nu)$. It is clear from (13) that the output error bound $\Delta_N^s(t^k; \nu)$ can be directly evaluated in terms of the dual norm of $\ell$ — which we can readily compute in the Construction stage — and the $L^2(\Omega)$ error bound, $\Delta_N^k(\nu)$; we thus focus on the $L^2(\Omega)$ error bound, $\Delta_N^k(\nu)$. It is furthermore clear from (20) that there are two components to the calculation of $\Delta_N^k(\nu)$: evaluation of $\rho_N^{\mathrm{LB}}(t^k; \nu)$ by the Successive Constraint Method, and computation of the dual norm of the residual, $\varepsilon_N(t^k; \nu)$ of (15). We first briefly discuss the Construction–Evaluation decomposition for the former; we then consider the latter (computation of the dual norm for quadratic nonlinearities is described in detail in [32, 24], and we thus provide here only a brief summary).

In the Construction stage of the SCM we form the sets $\mathcal{B}_N$ and $\{\rho_N(\mu') \mid \mu' \in \mathcal{C}_J\}$ for the lower bound and the set $\{y^*(\mu') \mid \mu' \in \mathcal{C}_J\}$ for the upper bound. Clearly, the operation count for this Construction stage is dependent on $\mathcal{N}$ — and quite intensive: we must compute many finite element minimum eigenvalues and eigenvectors. In the Evaluation stage of the SCM, both the lower bound and upper bound calculations are quite simple, as already described in Section 3: the lower bound is a small Linear Program; the upper bound is an enumeration/comparison. (In both cases, we must first find the $M$ closest points to $\mu$ in $C_{J^{\max}}$ — from (41) — to form $C_{J^{\max}}^{M,\mu}$: this is readily effected by a simple sort.) The storage and operation count in the Evaluation stage is independent of $\mathcal{N}$, and in fact typically quite small relative to other components.

We now turn to the dual norm of the residual. We first note from duality that $\varepsilon_N(t^k; \nu)$ can be expressed as

$$\varepsilon_N^2(t^k; \nu) = \|\hat{e}_N(t^k; \nu)\|_X^2, \quad 1 \leq k \leq K, \qquad (56)$$

where $\hat{e}_N(t^k; \nu)$ is the Riesz representation of the residual,

$$(\hat{e}_N(t^k; \nu), v)_X = r_N(v; t^k; \nu), \quad \forall v \in X^{\mathcal{N}}. \qquad (57)$$

Here $r_N(v; t^k; \nu)$ is the residual defined in (16), which we may further write — exploiting the reduced basis representation — as

$$r_N(v; t^k; \nu) = f(v) - \frac{1}{\Delta t} \sum_{j=1}^{N} (\omega_{N\,j}^k(\nu) - \omega_{N\,j}^{k-1}(\nu))(\xi_j, v)$$
$$- \sum_{n=1}^{N} \sum_{j=1}^{N} \omega_{N\,n}^k(\nu) \omega_{N\,j}^k(\nu) c(\xi_n, \xi_j, v) - \nu \sum_{j=1}^{N} \omega_{N\,j}^k(\nu) a(\xi_j, v), \tag{58}$$

for $1 \le k \le K$.

It now follows directly from (57) and (58) that

$$\hat{e}_N(t^k; \nu) = \sum_{m=1}^{(N+1)^2} \Upsilon_N^m(t^k; \nu) \Gamma_N^m, \quad 1 \le k \le K, \tag{59}$$

where the $\Upsilon_N^m(t^k; \nu)$ depend on timestep and viscosity $\nu$ explicitly but also through $\omega(t^k; \nu)$ and $\omega(t^{k-1}; \nu)$, and the $\Gamma_N^m$ are solutions to time–independent and $\nu$–independent "Poisson" problems of the form

$$(\Gamma_N^m, v)_X = g_N^m(v), \quad \forall v \in X^{\mathcal{N}}. \tag{60}$$

The $\Upsilon_N^m(t^k; \nu), g_N^m, 1 \le m \le (N+1)^2$, are given (for a particular ordering) by

$$\Upsilon_N^1(t^k; \nu) = 1, \Upsilon_N^2(t^k; \nu) = -\frac{(\omega_{N\,1}^k - \omega_{N\,1}^{k-1})}{\Delta t}, \dots,$$
$$\Upsilon_N^{N+2}(t^k; \nu) = \omega_{N\,1}^k(\nu) \omega_{N\,1}^k(\nu), \dots, \Upsilon_N^{N^2+2N+1} = -\nu \tag{61}$$

corresponding to

$$g_N^1(v) = f(v), g_N^2 = (\xi_1, v), \dots, g_N^{N+2}(v) = c(\xi_1, \xi_1, v) \dots, g_N^{N^2+2N+1}(v) = a(\xi_N, v). \tag{62}$$

It then follows from (56) that

$$\varepsilon_N^2(t^k; \nu) = \sum_{i=1}^{(N+1)^2} \sum_{j=1}^{(N+1)^2} \Upsilon_N^i(t^k; \nu) \Upsilon_N^j(t^k; \nu) (\Gamma_N^i, \Gamma_N^j)_X, \quad 1 \le k \le K. \tag{63}$$

The Construction–Evaluation decomposition is now clear.

In the *Construction* stage, we find the $\Gamma_{N_{\max}}^m, 1 \le m \le (N_{\max} + 1)^2$, and form the inner products $(\Gamma_{N_{\max}}^i, \Gamma_{N_{\max}}^j)_X, 1 \le i, j \le (N_{\max} + 1)^2$. The operation count for the Construction stage clearly depends on $\mathcal{N}$ — $(N_{\max}+1)^2$ finite element "Poisson" problems (60) and $(N_{\max}+1)^4$ finite element quadratures over the triangulation. (The temporary storage associated with the latter can be excessive for higher–dimensional problems: it is simple to develop procedures that balance temporary storage and re–computation.) Note that, thanks to the hierarchical nature of the reduced basis spaces, the inner products $(\Gamma_N^i, \Gamma_N^j)_X, 1 \le i, j \le (N+1)^2$, for any $N \le N_{\max}$ can be directly extracted from the corresponding $N_{\max}$ quantities. (As already noted, for nonhierarchical reduced basis spaces the storage requirements will be considerably higher.)

In the *Evaluation* stage, given the reduced basis coefficients $\omega_{N\,j}(t^k; \nu), 1 \le j \le N, 1 \le k \le K$: we can readily compute the coefficient functions $\Upsilon_N^j(t^k; \nu), 1 \le j \le (N+1)^2, 1 \le k \le K$; we then simply perform the sum (63) from the stored inner products — $O((N+1)^4)$ operations per time step and hence $O((N+1)^4 K)$ operations in total. As desired, the operation count for the Evaluation stage is indeed independent of $\mathcal{N}$. The quartic scaling with $N$ is obviously less than welcome, however in actual practice for modest $N$ the cost to evaluate $s(t^k; \nu)$ and the

cost to evaluate $\Delta_N(t^k; \nu)$ are often commensurate — the many $O(N^3)$ operations of the former typically balance the $(N+1)^4$ operations of the latter.

This concludes the discussion of the Construction–Evaluation decomposition. The Construction stage is performed Offline; the Evaluation stage is invoked Online — for each new $\nu$ of interest in the real–time or many–query contexts. However, there are two other components to the Offline stage. First, we must construct a good (rapidly convergent) reduced basis space and associated basis functions $\xi_i, 1 \leq i \leq N_{\max}$; this sampling process in fact relies on the Construction–Evaluation decomposition to greatly reduce the requisite number of "candidate" finite element calculations. And second, we must construct our SCM "constraint sample" by the greedy procedure described in Section 3; this process also relies on the Construction–Evaluation decomposition, in particular for the (inexpensive) stability factor lower and upper bound calculations over the (extensive) SCM training sample. We shall focus our attention on the construction of the reduced basis space, as we have already described the corresponding SCM procedures.

*4.2. POD-Greedy Sampling Strategy*

We address here the generation of our RB space $X_N$. We follow [13] and combine the POD (Proper Orthogonal Decomposition) in $t^k$ — to capture the causality associated with our evolution equation — with the Greedy procedure [10,34,31] in $\nu$ — to treat efficiently the higher dimensions and more extensive ranges of parameter variation. To begin, we summarize the well-known optimality property of the POD [22]. Given $J$ elements of $X^{\mathcal{N}}$, $w_j \in X^{\mathcal{N}}, 1 \leq j \leq J$, and any positive integer $M \leq \mathcal{N}$, POD$(\{w_1, \ldots, w_J\}, M)$ returns $M$ $(\cdot, \cdot)_X$-orthonormal functions $\{\chi_m, 1 \leq m \leq M\}$ such that the space $\mathcal{P}_M = \operatorname{span}\{\chi_m, 1 \leq m \leq M\}$ is optimal in the sense that

$$\mathcal{P}_M = \arg \inf_{Y_M \subset \operatorname{span}\{w_j, 1 \leq j \leq J\}} \left( \frac{1}{J} \sum_{j=1}^{J} \inf_{v \in Y_M} \|w_j - v\|_X^2 \right)^{1/2},$$

where $Y_M$ denotes an $M$-dimensional linear space.

To initiate the POD-Greedy sampling procedure we must specify a very large (exhaustive) "train" sample of $n_{\text{train}}$ points in $\mathcal{D}$, $\Xi_{\text{train}}$, and an initial (say, random) sample $S^* = \{\nu_0^*\}$. Moreover, we shall require a nominal value $\rho_N^*$ for the lower bound of the stability constant: for the purposes of the POD-Greedy sampling *only*, we replace our SCM lower bound with $\rho_N^{\text{LB}}(t^k; \nu) = \rho_N^*, 1 \leq k \leq K, \forall \nu \in \mathcal{D}$; we then define $\Delta_N^*(t^k; \nu)$ to be our usual *a posteriori* error bound but now for the "nominal" stability factor $\rho_N^*$ — hence $\Delta_N^*(t^k; \nu)$ is not in fact a true error *bound* but rather just an indicator. (We return to this point at the conclusion of this section.)

The algorithm is then given by

> Set $\mathcal{Z} = \emptyset$;
>
> Set $\nu^* = \nu_0^*$;
>
> While   $N \leq N_{\max}$
>
> > $\{\chi_m, 1 \leq m \leq M_1\} = \text{POD}(\{u^{\mathcal{N}}(t^k, \nu^*), 1 \leq k \leq K\}, M_1)$ ;
> >
> > $\mathcal{Z} \leftarrow \{\mathcal{Z}, \{\chi_m, 1 \leq m \leq M_1\}\}$ ;
> >
> > $N \leftarrow N + M_2$ ;
> >
> > $\{\xi_n, 1 \leq n \leq N\} = \text{POD}(\mathcal{Z}, N)$ ;
> >
> > $X_N = \text{span}\{\xi_n, 1 \leq n \leq N\}$ ;
> >
> > $\nu^* = \arg\max_{\nu \in \Xi_{\text{train}}} \Delta_N^*(t^K = T; \nu)$
> >
> > $S^* \leftarrow \{S^*, \nu^*\}$ ;
>
> end.
>
> Set $X_N = \text{span}\{\xi_n, 1 \leq n \leq N\}, 1 \leq N \leq N_{\max}$.

In actual practice, we typically exit the POD-Greedy sampling procedure at $N = N_{\max} \leq N_{\max,0}$ for which a prescribed error tolerance is satisfied: to wit, we define

$$\epsilon_{N,\max}^* = \max_{\nu \in \Xi_{\text{train}}} \Delta_N^*(t^K; \nu),$$

and terminate when $\epsilon_{N,\max}^* \leq \epsilon_{\text{tol}}^*$. Note by virtue of the final re–definition the POD-Greedy generates *hierarchical* spaces $X_N$, $1 \leq N \leq N_{\max}$, which is computationally very advantageous.

There are two "tuning" variables in the POD-Greedy procedure, $M_1$ and $M_2$. We choose $M_1$ to satisfy an internal POD error criterion based on the usual sum of eigenvalues; we choose $M_2 \leq M_1$ to minimize duplication in the RB space. It is important to note that the POD–Greedy method readily accommodates a repeat $\nu^*$ in successive Greedy cycles — new information will always be available and old information rejected; in contrast, a pure Greedy approach in both $t$ and $\nu$ [10], though often generating good spaces, can "stall." Furthermore, since the POD is conducted in only one (time) dimension — with the Greedy addressing the remaining (para-meter) dimensions — the procedure remains computationally feasible even for large parameter domains and very extensive parameter train samples (and in particular in higher parameter dimensions). We now discuss the computational aspects in slightly more detail.

The crucial point to note is that the operation count for POD-Greedy algorithm is addi-tive and not multiplicative in $n_{\text{train}}$ and $\mathcal{N}$. In particular, in searching for the next parameter value $\nu^*$, we invoke the Construction–Evaluation decomposition to inexpensively calculate the *a posteriori* error bound at the $n_{\text{train}}$ candidate parameter values. In contrast, in a pure POD approach, we would need to evaluate the finite element "truth" solution at the $n_{\text{train}}$ candidate parameter values. (Of course, much of the computational economies are due not to the Greedy *per se*, but rather to the accommodation within the Greedy of the inexpensive error bounds.) As a result, in the POD-Greedy approach we can take $n_{\text{train}}$ relatively large: we can thus anticipate reduced basis spaces and approximations that provide rapid convergence *uniformly* over the entire parameter domain. (Note that more sophisticated and hence efficient search algorithms can be exploited in the Greedy context, for example [2].)

Once the reduced basis spaces are defined we can then construct our SCM lower bound for the stability factor. If we find that the true lower bound is in fact very different from — much more negative than — our nominal value $\rho_N^*$ we may wish to, or need to, return to the POD–Greedy algorithm in order to ensure a sufficiently accurate reduced basis approximation. Typically if we choose $\rho_N^*$ and $\epsilon_{\text{tol}}^*$ conservatively such a "restart" is not required. It is imperative

(a) $\nu = 0.005$

(b) $\nu = 0.01$

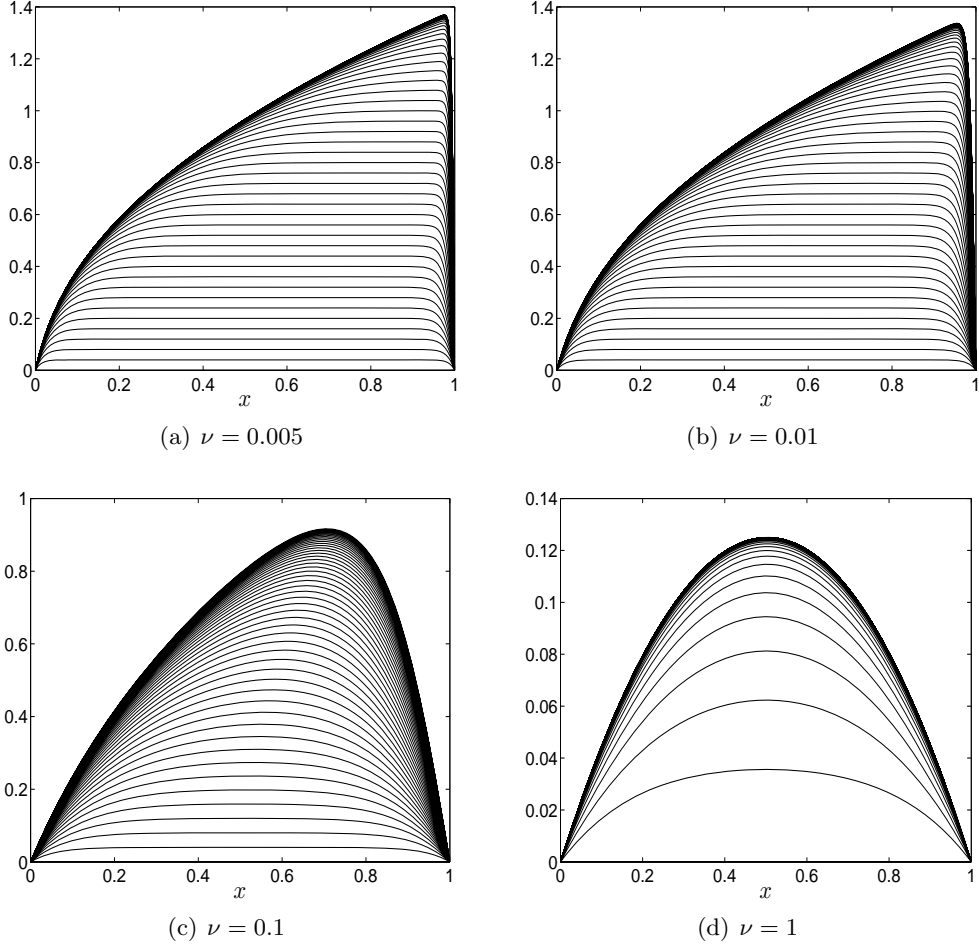(c) $\nu = 0.1$

(d) $\nu = 1$

**Fig. 1.** Solution of the Burgers equation $u^{\mathcal{N}}(x, t^k; \nu)$ as a function of $x$ and $t^k$: (a) $\nu = 0.005$, (b) $\nu = 0.01$, (c) $\nu = 0.1$, and (d) $\nu = 1$.

to note that, in actual Online calculations — evaluations $\mu \to s_N(t^k; \nu), \Delta_N^{s\,k}(\mu)$ in many–query and real–time applications such as optimization, control, and parameter estimation — we rely on the true stability factor lower bound such that Propositions 1 and 2 are rigorously valid. (Note also that the $\mathcal{N}$-independence of the Evaluation/Online stage permits us to choose our $\mathcal{N}$ conservatively — thus ensuring a highly accurate "truth.")

## 5. Numerical results

We consider the time interval $[0, T]$ with $T = 2$ and viscosity range $\mathcal{D} = [\nu_{\min}, \nu_{\max}]$ with $\nu_{\min} = 0.005$ and $\nu_{\max} = 1$. For the truth approximation we consider a regular mesh of $\mathcal{N} = 401$ degrees of freedom and a constant timestep $\Delta t = 0.02$ corresponding to $K = 100$ time steps. We present in Figure 1 the truth solution of the time-dependent viscous Burger problem as a function of space and time for $\nu = 1, \nu = 0.1, \nu = 0.01$, and $\nu = 0.005$: the field evolves to a steady state with outer solution $\sqrt{2x}$ and inner boundary layer (at $x = 1$) of thickness $\nu$. (We have confirmed that all the results presented in this section are insensitive to (further increases) in $\mathcal{N}$.)

We next choose a log uniformly distributed sample $\Xi_{\text{train}} = \Xi_{\text{train,SCM}}$ of size $n_{\text{train}} = 50$ and pursue the POD-Greedy sampling procedure with $\rho_N^* = 0$, $\nu_0^* = 0.005$, and $\epsilon_{\text{tol}}^* = 10^{-3}$. The POD-Greedy sampling terminates after 6 POD–greedy iterations — one iteration is defined as
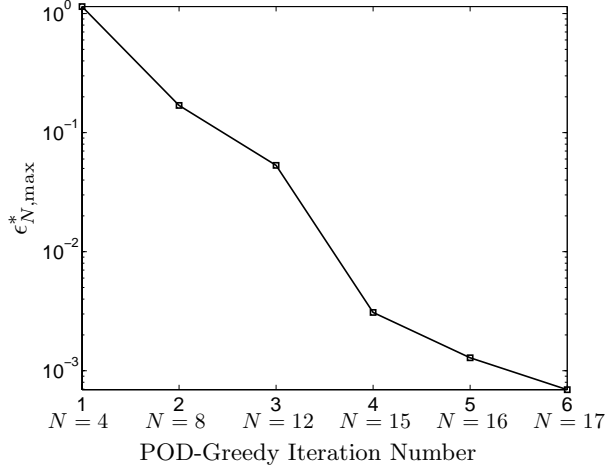
**Fig. 2.** The error indicator $\epsilon^*_{N,\max}$ as a function of POD-greedy iteration number and also $N$.

one pass through the While loop — and yields $N_{\max} = 17$ and the optimal parameter sample

$$S^* = [0.0050, 0.0365, 0.0107, 0.1424, 0.0057, 0.0065, 0.0074].$$

We observe, not surprisingly, that most of the POD–Greedy sample points are close to $\nu_{\min} = 0.005$. We present in Figure 2 $\epsilon^*_{N,\max}$ as a function of POD-greedy iteration number (and $N$). Clearly, the error indicator $\epsilon^*_{N,\max}$ decreases very rapidly with $N$; we shall subsequently confirm that the rigorous error bound, and hence also the true error, also decreases very rapidly with $N$.

We now turn to the stability factor. For the same training sample we perform the SCM procedure to construct the lower bound for the stability factor. We present in Figure 3 the SCM sample $\mathcal{C}_J$ for $J = J^{\max} = 80$; we see that most of the sample points are close to $\nu_{\min} = 0.005$, and that many sample points correspond to the final time $T = 2$. Note that $J^{\max}$ is less than $K$ (and of course much less than $Kn_{\text{train,SCM}}$) and hence the SCM is clearly providing substantial approximation in (discrete) time and (continuous) parameter. Of course the (POD–Greedy) reduced basis approximation $u_N(t^k; \nu)$ will converge much more rapidly to $w^{\mathcal{N}}(t^k; \nu)$ in $N$ than the (Greedy) SCM approximation $\rho_N^{LB}(t^k; \nu)$ will converge to $\rho_N(t^k; \nu)$ in $J$: the reduced basis projection exploits smoothness in parameter and Galerkin optimality, whereas the SCM construction — focused on a lower bound — enlists only rather weak constraints and low–order interpolation. Fortunately, whereas we require a highly accurate reduced basis approximation, we are content with a relatively crude stability factor; note also that whereas the reduced basis Online operation count depends on $N$, the SCM Online operation count depends on $M$ — here $M = 16$ — and not $J^{\max}$.

We now present in Figure 4 the stability factor $\rho_N(t^k; \nu)$ as a function of $t^k$ for $\nu = 1, 0.1, 0.01$, and 0.005 for $N = 17$; we also present the stability factor lower bound $\rho_N^{\text{LB}}(t^k; \nu)$ as well as a corresponding upper bound $\rho_N^{\text{UB}}(t^k; \nu)$. As already indicated, $\rho_N(t^k; \nu)$ reflects the detailed spatial and temporal structure of $u_N^k(\nu), 1 \le k \le K$, as well as viscous stabilization effects. As a result, even for $\nu = 0.005$ — clearly a convectively–dominated highly nonlinear flow — $\rho_N(t^k; \nu)$ is still mostly positive (stable): in our particular example, $u_N^k(\nu)$ is "dangerous" only within the boundary layer. It should also be noted that the SCM method yields a very good upper bound for the stability factor (and significantly less complicated and less costly than a standard reduced basis Rayleigh–Ritz aproximation): the difference between $\rho_N^{\text{UB}}(t^k; \nu)$ and $\rho_N(t^k; \nu)$ is indeed very small. (If we replace $\rho_N^{\text{LB}}(t^k; \nu)$ with $\rho_N^{\text{UB}}(t^k; \nu)$ in (20) we will certainly obtain better error bounds — but we can no longer provide rigorous guarantees.)

Finally, we present in Figure 5 the actual $L^2(\Omega)$ error, $\|w^{\mathcal{N}}(\cdot, t^k; \nu) - u_N(\cdot, t^k; \nu)\|$, and the error bound $\Delta_N(t^k; \nu)$ as a function of discrete time $t^k$ for $N = 5, 10$, and 15 and for
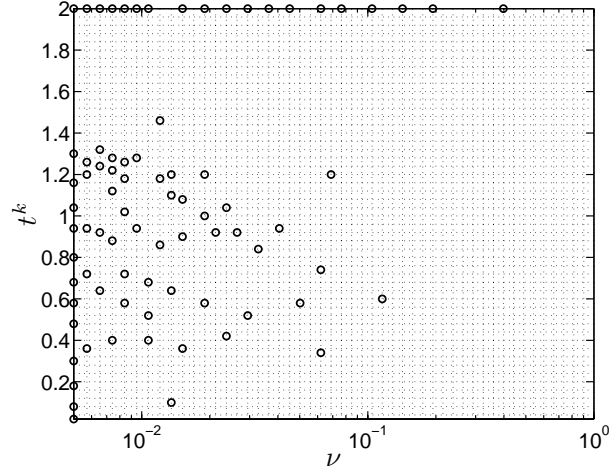
**Fig. 3.** Distribution of the SCM sample $\mathcal{C}_J$ in time domain (linear scale) and parameter domain (log scale). Note each horizontal gray line corresponds to a $t^k$, $k = 2, 4, ..., K$, and each vertical gray line corresponds to a point in $\Xi_{\text{train,SCM}}$.



(a) $\nu = 0.005$

(b) $\nu = 0.01$

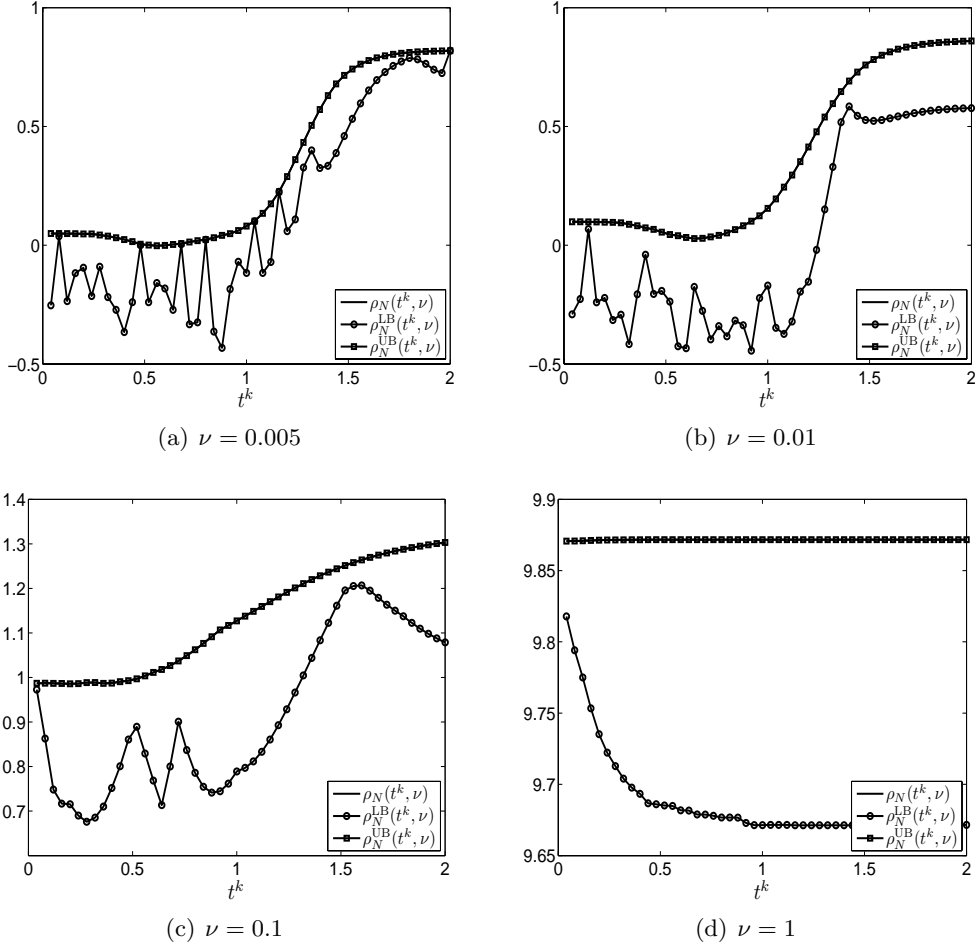(c) $\nu = 0.1$

(d) $\nu = 1$

**Fig. 4.** Stability factors $\rho_N(t^k; \nu)$, $\rho_N^{\text{LB}}(t^k; \nu)$, and $\rho_N^{\text{UB}}(t^k; \nu)$ as a function of $t^k$ for $N = 17$: (a) $\nu = 0.005$, (b) $\nu = 0.01$, (c) $\nu = 0.1$, and (d) $\nu = 1$.

$\nu = 0.005, 0.01, 0.1$, and 1. Figure 6 provides the output error , $|s^{\mathcal{N}}(t^k; \nu) - s_N(t^k; \nu)|$ and the output error bound $\Delta_N^s(t^k; \nu)$ for the same values of $N$ and $\nu$. We observe that the reduced basis approximation converges quite rapidly, and that furthermore the *a posteriori* error bound $\Delta_N(t^k; \nu)$ is (rigorous, but also) reasonably sharp. Indeed, even for $\nu = 0.005$, the numerical approximation and associated *a posteriori* error estimators are both still quite good for times of order unity. However, the output error bound $\Delta_N^s(t^k; \nu)$ is not as sharp as the $L^2$ error bound $\Delta_N(t^k; \nu)$: the output effectivity $\eta_N^s(t^k; \nu)$ can be as large as $O(1000)$, whereas the $L^2$ effectivity $\eta_N(t^k; \nu)$ is only $O(10)$; we believe that the sharpness of the output error bound can be significantly improved by introduction of adjoint techniques [20, 25] — this development will be pursued in future work.

In summary, for $\nu$ very small — Reynolds number very large — and for long times $T$ our *a posteriori* error bounds *will no longer be useful*. However, viscosities $\nu = .005$ (Reynolds numbers $O(200)$) and moderate times can be of significant practical import: there are a variety of new microtechnology–related flows which occur at relatively low Reynolds number; furthermore, for some turbulent situations in which smaller scales can be eliminated/modelled the *effective* Reynolds number is modest. Further work is required to determine if the theory and methodology can be extended sufficiently — in particular, to the full incompressible Navier–Stokes equations — to treat problems relevant to engineering practice.
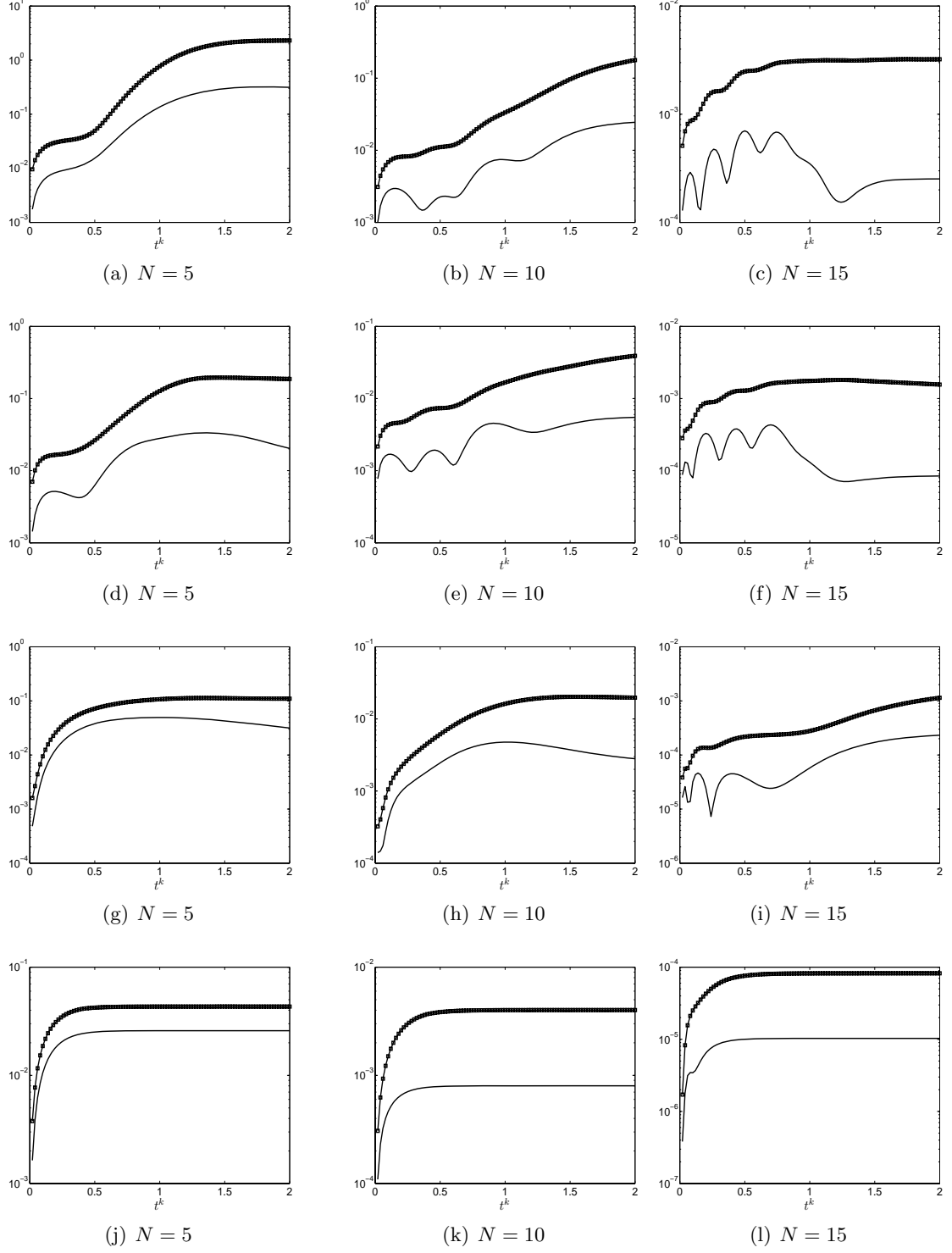
(a) $N = 5$  (b) $N = 10$  (c) $N = 15$

(d) $N = 5$  (e) $N = 10$  (f) $N = 15$

(g) $N = 5$  (h) $N = 10$  (i) $N = 15$

(j) $N = 5$  (k) $N = 10$  (l) $N = 15$

**Fig. 5.** The actual $L^2(\Omega)$ error, $\|u^{\mathcal{N}\,k}(\nu) - u_N^k(\nu)\|$ (solid line), and the $L^2$ error bound, $\Delta_N^k(\nu)$ (square symbol), as a function of discrete time $t^k$ for $N = 5, 10$, and 15 and for $\nu = 0.005$ (top row), $\nu = 0.01$ (second row), $\nu = 0.1$ (third row), and $\nu = 1$ (bottom row).
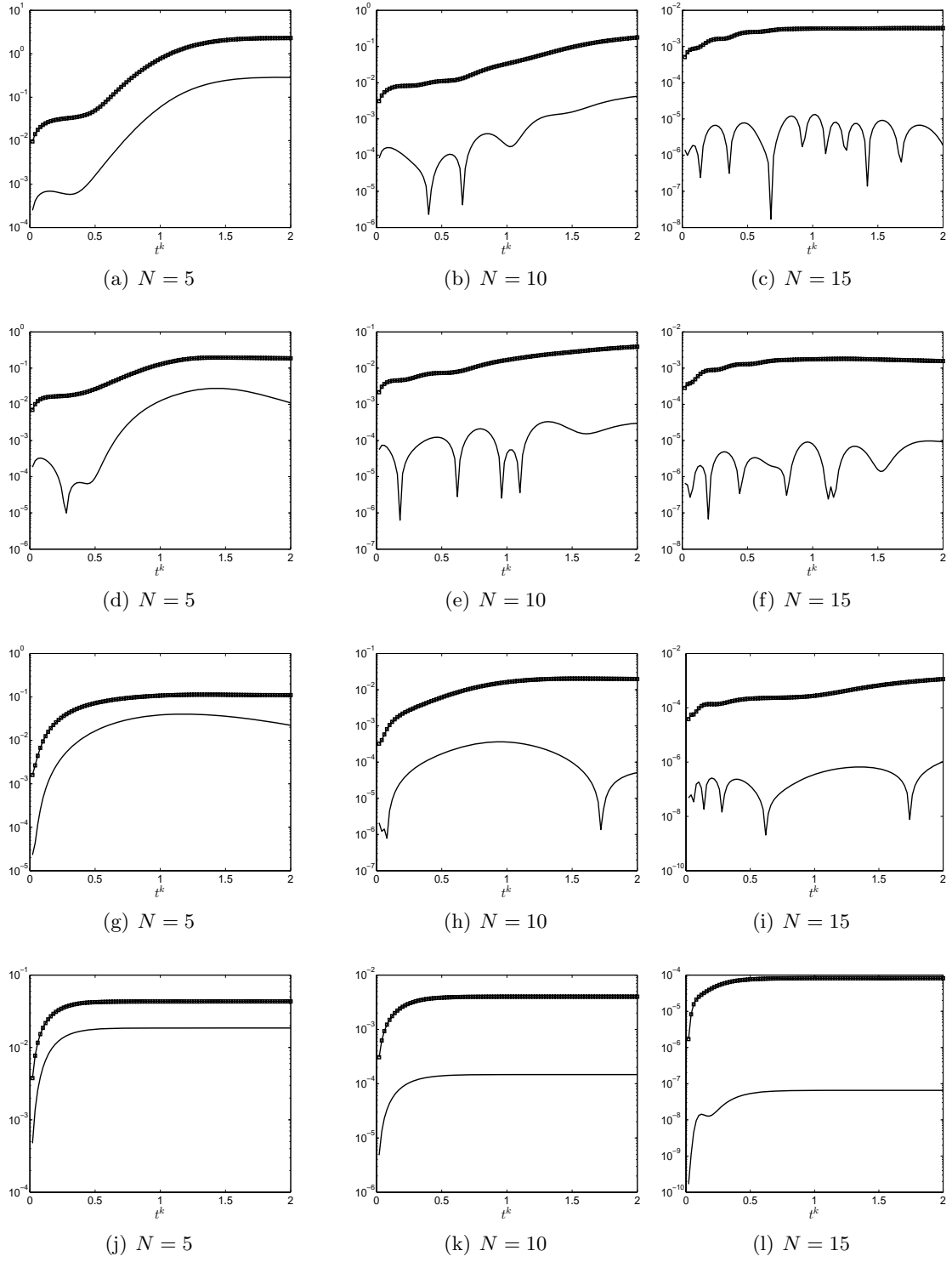
19

**Fig. 6.** The output error, $|s^{\mathcal{N}\,k}(\nu) - s_N^k(\nu)|$ (solid line), and the output error bound, $\Delta_N^{s\,k}(\nu)$ (square symbol), as a function of discrete time $t^k$ for $N = 5, 10$, and 15 and for $\nu = 0.005$ (top row), $\nu = 0.01$ (second row), $\nu = 0.1$ (third row), and $\nu = 1$ (bottom row).

# References

1. Barrault, M., Nguyen, N.C., Maday, Y., Patera, A.T.: An "empirical interpolation" method: Application to efficient reduced-basis discretization of partial differential equations. C. R. Acad. Sci. Paris, Série I. **339**, 667–672 (2004)

2. Bui-Thanh, T., Willcox, K., Ghattas, O.: Model reduction for large-scale systems with high-dimensional parametric input space (AIAA Paper 2007-2049). In: Proceedings of the 48th AIAA/ASME/ASCE/AHS/ASC Structures, Structural Dynamics and Material Conference (2007)

3. Burkardt, J., Gunzburger, M.D., Lee, H.C.: Pod and cvt-based reduced order modeling of Navier-Stokes flows. Comp. Meth. Applied Mech. **196**, 337–355 (2006)

4. Cancès, E., Le Bris, C., Nguyen, N.C., Maday, Y., Patera, A.T., Pau, G.S.H.: Feasibility and competitiveness of a reduced basis approach for rapid electronic structure calculations in quantum chemistry. In: Proceedings of the Workshop for High-dimensional Partial Differential Equations in Science and Engineering (Montreal), vol. 41, pp. 15–57 (2007)

5. Christensen, E.A., Brons, M., Sorensen, J.N.: Evaluation of pod-based decomposition techniques applied to parameter-dependent non-turbulent flows. SIAM J. Sci. Comput. **21**, 1419 (2000)

6. Constantin, P., Foias, C.: Navier-Stokes Equations. Chicago Lectures in Mathematics. University of Chicago Press, Chicago, IL (1988)

7. Deane, A., Kevrekidis, I., Karniadakis, G., Orszag, S.: Low-dimensional models for complex geometry flows: Application to grooved channels and circular cylinders. Phys. Fluids **10**, 2337–2354 (1991)

8. Grepl, M.: Reduced-basis approximations and *a posteriori* error estimation for parabolic partial differential equations. Ph.D. thesis, Massachusetts Institute of Technology (2005)

9. Grepl, M.A., Maday, Y., Nguyen, N.C., Patera, A.T.: Efficient reduced-basis treatment of nonaffine and nonlinear partial differential equations. M2AN (Math. Model. Numer. Anal.) **41**(2), 575–605 (2007). (Doi: 10.1051/m2an:2007031)

10. Grepl, M.A., Patera, A.T.: *A Posteriori* error bounds for reduced-basis approximations of parametrized parabolic partial differential equations. M2AN (Math. Model. Numer. Anal.) **39**(1), 157–181 (2005)

11. Gunzburger, M.D.: Finite Element Methods for Viscous Incompressible Flows. Academic Press (1989)

12. Gunzburger, M.D., Peterson, J., Shadid, J.N.: Reduced-order modeling of time-dependent PDEs with multiple parameters in the boundary data. Comp. Meth. Applied Mech. **196**, 1030–1047 (2007)

13. Haasdonk, B., Ohlberger, M.: Reduced basis method for finite volume approximations of parametrized linear evolution equations. Mathematical Modelling and Numerical Analysis (M2AN) **42**(3), 277–302 (2008). (Doi: 10.1051/m2an:2008001)

14. Huynh, D.B.P., Rozza, G., Sen, S., Patera, A.T.: A successive constraint linear optimization method for lower bounds of parametric coercivity and inf-sup stability constants. C. R. Acad. Sci. Paris, Analyse Numérique **345**(8), 473–478 (2007). (doi: 10.1016/j.crma.2007.09.019)

15. Ito, K., Ravindran, S.S.: A reduced basis method for control problems governed by PDEs. In: W. Desch, F. Kappel, K. Kunisch (eds.) Control and Estimation of Distributed Parameter Systems, pp. 153–168. Birkhäuser (1998)

16. Ito, K., Ravindran, S.S.: A reduced-order method for simulation and control of fluid flows. Journal of Computational Physics **143**(2), 403–425 (1998)

17. Ito, K., Ravindran, S.S.: Reduced basis method for optimal control of unsteady viscous flows. International Journal of Computational Fluid Dynamics **15**(2), 97–113 (2001)

18. Ito, K., Schroeter, J.D.: Reduced order feedback synthesis for viscous incompressible flows. Mathematical And Computer Modelling **33**(1-3), 173–192 (2001)

19. Johansson, P.S., Andersson, H., Rønquist, E.: Reduced-basis modeling of turbulent plane channel flow. Computers and Fluids **35**(2), 189–207 (2006)

20. Johnson, C., Rannacher, R., Boman, M.: Numerical and hydrodynamic stability: Towards error control in computational fluid dynamics. SIAM Journal of Numerical Analysis **32**(4), 1058–1079 (1995)

21. Joseph, D.: Stability of fluid motions. I. & II., *Springer Tracts in Natural Philosophy*, vol. 27 & 28. Springer-Verlag, New York (1976)

22. Kunisch, K., Volkwein, S.: Galerkin proper orthogonal decomposition methods for a general equation in fluid dynamics. SIAM J. Num. Analysis **40**(2), 492–515 (2002)

23. LeVeque, R.J.: Numerical Methods for Conservation Laws. Lectures in Mathematics, ETH-Zurich. Birkhauser-Verlag, Basel (1990)

24. Nguyen, N.C., Veroy, K., Patera, A.T.: Certified real-time solution of parametrized partial differential equations. In: S. Yip (ed.) Handbook of Materials Modeling, pp. 1523–1558. Springer (2005)

25. Pierce, N., Giles, M.B.: Adjoint recovery of superconvergent functionals from PDE approximations. SIAM Review **42**(2), 247–264 (2000)

26. Porsching, T.A., Lee, M.Y.L.: The reduced-basis method for initial value problems. SIAM Journal of Numerical Analysis **24**, 1277–1287 (1987)

27. Prud'homme, C., Rovas, D., Veroy, K., Maday, Y., Patera, A., Turinici, G.: Reliable real-time solution of parametrized partial differential equations: Reduced-basis output bounds methods. Journal of Fluids Engineering **124**(1), 70–80 (2002)
28. Quarteroni, A., Rozza, G.: Numerical solution of parametrized Navier-Stokes equations by reduced basis method. Num. Meth. PDEs **23**, 923–948 (2007)
29. Quarteroni, A., Valli, A.: Numerical Approximation of Partial Differential Equations, 2nd edn. Springer (1997)
30. Rovas, D., Machiels, L., Maday, Y.: Reduced basis output bounds methods for parabolic problems. IMA J. Appl. Math. **26**, 423–445 (2006)
31. Rozza, G., Huynh, D.B.P., Patera, A.T.: Reduced basis approximation and a posteriori error estimation for affinely parametrized elliptic coercive partial differential equations: Application to transport and continuum mechanics. Archives Computational Methods in Engineering **15**(4) (2008)
32. Veroy, K., Patera, A.T.: Certified real-time solution of the parametrized steady incompressible Navier-Stokes equations; Rigorous reduced-basis a posteriori error bounds. International Journal for Numerical Methods in Fluids **47**, 773–788 (2005)
33. Veroy, K., Prud'homme, C., Patera, A.T.: Reduced-basis approximation of the viscous Burgers equation: Rigorous a posteriori error bounds. C. R. Acad. Sci. Paris, Série I **337**(9), 619–624 (2003)
34. Veroy, K., Prud'homme, C., Rovas, D.V., Patera, A.T.: A Posteriori error bounds for reduced-basis approximation of parametrized noncoercive and nonlinear elliptic partial differential equations. In: Proceedings of the 16th AIAA Computational Fluid Dynamics Conference (2003). Paper 2003-3847